JOC The Journal of Organic Chemistry

Article

pubs.acs.org/joc

Organocatalytic Preparation of Substituted Cyclopentanes: A Mechanistic Study

Alexandra Tsybizova, Marek Remeš, Jan Veselý, Simona Hybelbauerová, and Jana Roithová*

Department of Organic Chemistry, Faculty of Science, Charles University in Prague, Hlavova 2030/8, 12843 Prague 2, Czech Republic

Supporting Information

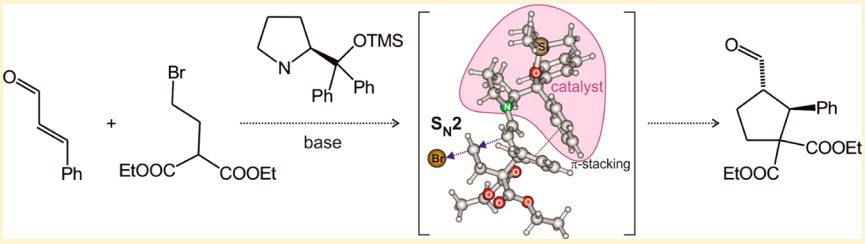

ABSTRACT: The reaction mechanism of a tandem conjugate addition/α-alkylation of enals leading to functionalized cyclopentanes catalyzed by *O*-trimethylsilyldiphenylprolinol was investigated by mass spectrometry, NMR spectroscopy, and DFT calculations. We have shown that the high stereoselectivity of the reaction depends on the energy discrimination between the two stereoisomers formed by the condensation of the α,β-unsaturated aldehyde (cinnamaldehyde) and the catalyst. The stereoselectivity of this step depends on the solvent used. The experimental activation barriers were determined to be $E_a = 25 \pm 7$ kJ mol^{-1} (Arrhenius equation), $\Delta H^{\ddagger} = 23 \pm 7$ kJ mol^{-1}, and $\Delta G^{\ddagger} = 101 \pm 9$ kJ mol^{-1} (Eyring equation).

INTRODUCTION

One of the domains of organocatalysis is represented by tandem or cascade reactions proceeding via iminium−enamine intermediates.[1] This type of organocatalytic cascade has been successfully applied for the formation of various cycles, such as aziridines, cyclopropanes, cyclopentanes, and others. The first enantioselective preparation of cyclopentane derivatives, namely, 2,3,4-trisubstituted cyclopentanones, via the above-mentioned cascade process was developed by Córdova in 2007.[2] The same group later developed another synthesis of cyclopentane derivatives based on a nitro-Michael/Michael sequence.[3] Shortly thereafter, Wang reported two other syntheses of cyclopentane derivatives that were initiated with a carbo-conjugated addition of malonates derivatives.[4,5] Other domino or cascade reactions leading to the formation of other highly functionalized cyclopentanes were developed by Enders and Ma.[6,7] All of the these methods include an intermolecular Michael addition step as the key step in a cascade process under catalysis with a chiral secondary amine. This strategy was expanded in a recently published protocol for the preparation of highly substituted cyclopentanes (Scheme 1) in which nonstabilized malonate-derived alkyl halides were used.[8] It has been shown that this reaction proceeds with high enantioselectivities and diastereoselectivities for various α,β-unsaturated aldehydes in a broad range of solvents.[8]

The suggested mechanism of this reaction starts with the formation of an adduct between the catalyst, *O*-trimethylsilyldiphenylprolinol (DPPTMS), and the α,β-unsaturated aldehyde (Figure 1). The resulting iminium intermediate reacts with deprotonated diethyl 2-(2-bromoethyl)malonate. The final step consists of closing the five-membered ring, which leads to the bromine anion and the iminium adduct of the catalyst with the product of the reaction. In principle, this reaction scheme could be also used for the synthesis of cyclohexanes or other cycloalkanes. Nevertheless, it has been shown that when the same reaction protocol is applied to an analogous reaction with diethyl 2-(3-bromopropyl)malonate and carried out under the same conditions it does not proceed at all. Hence, we were interested in the details of the reaction mechanism as well as the basis for the different results that stem from the prolongation of the bromoalkyl chain by one carbon atom.

Scheme 1. Investigated Organocatalytic Reaction

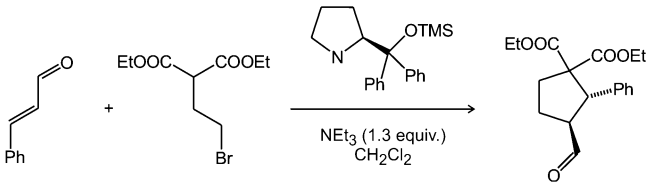

RESULTS AND DISCUSSION

Mass spectrometry coupled with electrospray ionization (ESI-MS) has been shown to be an efficient tool for the investigation of reaction mechanisms, where the reactants, products, and reaction intermediates are either charged as such or easily charged during ESI (protonated, deprotonated, or charged in

Received: October 4, 2013
Published: January 23, 2014

dx.doi.org/10.1021/jo4022106 | J. Org. Chem. 2014, 79, 1563−1570

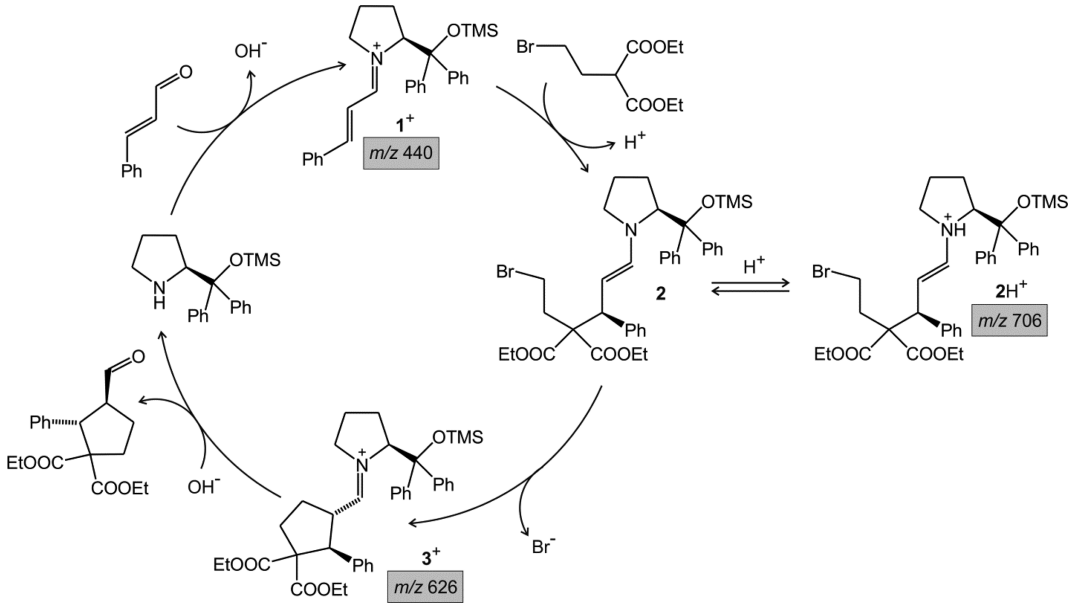

Figure 1. Suggested reaction mechanism and m/z ratios of the individual intermediates.

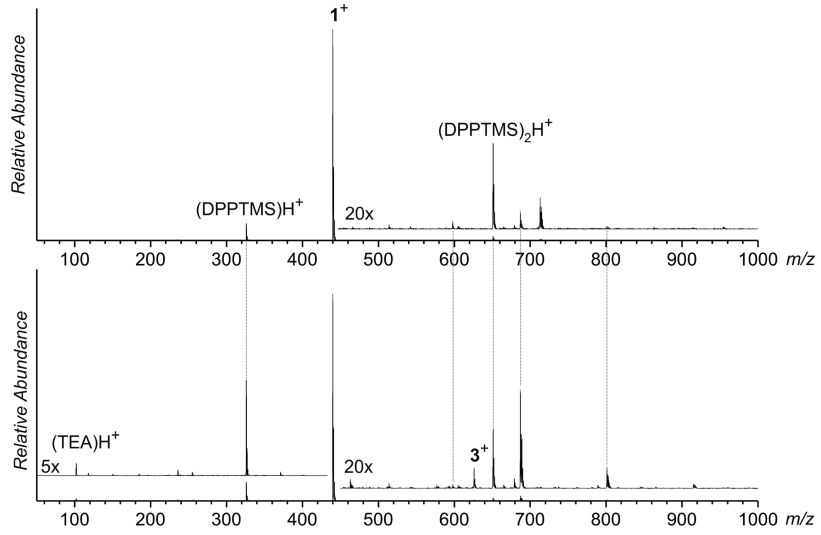

Figure 2. (a) ESI-MS spectrum of a 5 mM solution of cinnamaldelyde in CH_2Cl_2 with 20% DPPTMS catalyst. (b) ESI-MS spectrum of the same solution as in panel a but after addition of 1.1 equiv of diethyl 2-(2-bromoethyl)malonate and 1.3 equiv of triethylamine.

another way).[9−12] Such a situation is typical for organocatalytic reactions involving iminium or enamine catalysis.[13−19] Therefore, we investigated the reaction by means of ESI-MS.

First, we investigated the reaction mixture containing only cinnamaldehyde and catalyst DPPTMS (Figure 2a). The major peak in the spectrum is the iminium ion formed by the condensation of the catalyst with cinnamaldehyde (detection of analogous iminium ions by ESI-MS has been reported before, for example, in ref 14). Next to this peak, we can also see the protonated catalysts ($(DPPTMS)H^+$) and proton-bound dimers of the catalyst ($(DPPTMS)_2H^+$). Collision-induced dissociation (CID) of reactant complex $\mathbf{1}^+$ (Figure 3a) reveals that the dominant fragmentation of the iminium ions formed from the DPPTMS catalyst corresponds to the loss of the substituent group of the pyrrolidine ring. The diphenyltrimethylsilyloxymethyl group can either be eliminated as a cation (m/z 255) or the remaining part of the parent ion can remain charged (m/z 185). Minor fragmentations probably correspond to the elimination of 1-pyrroline (mass 69). This fragmentation must be associated with a transfer of the diphenyltrimethylsilyloxymethyl group to the former C(1) carbon of cinnamaldehyde (peak at m/z 371; see Scheme S1 in the Supporting Information). In a subsequent step, the formed ions can eliminate trimethylsilanol to yield an ion with m/z 281. This scenario was confirmed by MS^3 experiment in an ion trap (Figure S4 in the Supporting Information).

Addition of 1.1 equiv of diethyl 2-(2-bromoethyl)malonate does not lead to any change in the ESI-MS spectrum; hence, it is likely that no reaction takes place in the solution without the simultaneous addition of a base. In addition, during the electrospray ionization, we do not mimic the conditions for the reaction to occur. Therefore, to promote the reaction, we have added a base to the solution. We chose triethylamine, which gave lower yields in the preparative experiment compared to the other bases but is soluble in dichloromethane and therefore forms a homogeneous mixture suitable for the MS experiments.

dx.doi.org/10.1021/jo4022106 | J. Org. Chem. 2014, 79, 1563−1570

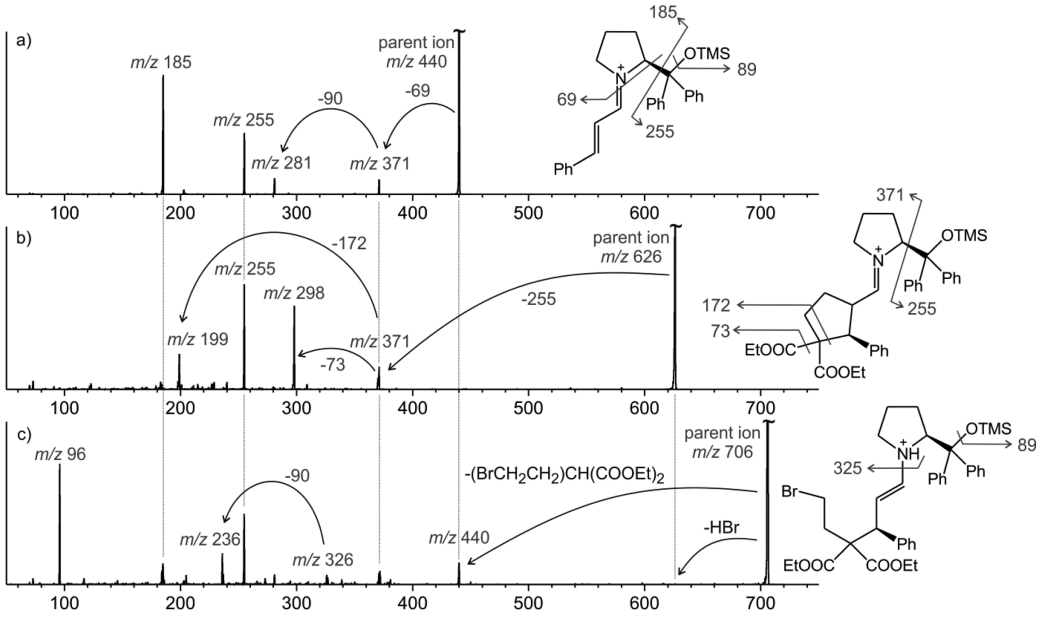

Figure 3. CID spectra of the iminium ions formed from the DPPTMS catalyst and (a) cinnamaldehyde or (b) the reaction product. (c) Protonated reaction intermediate after coupling between the iminium ion in panel a and diethyl 2-(2-bromoethyl)malonate. All ions were isolated from the reaction mixture that is specified in the Experimental Details.

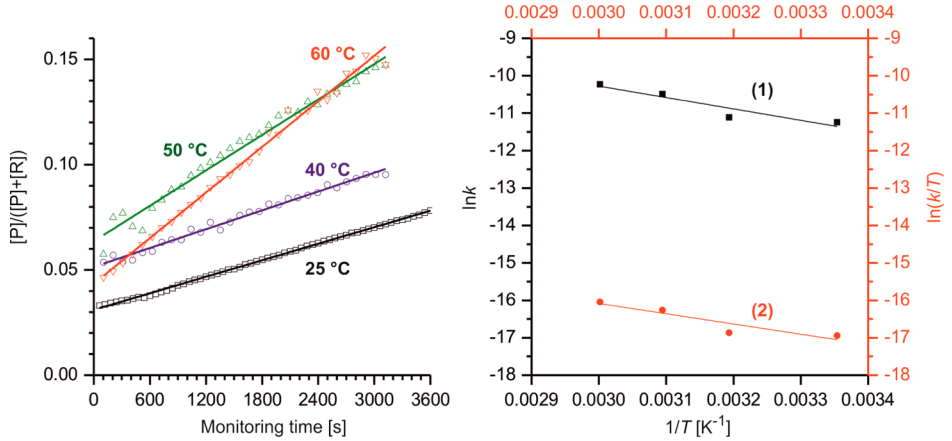

Figure 4. (a) Relative ratios of the products ($[P]/[R]_0 = [P]/([P] + [R])$) as functions of the reaction time monitored by NMR spectroscopy at different temperatures. (b) Determination of E_a according to the Arrhenius equation (denoted 1) and ΔH_{rxn} according to the Eyring equation (denoted 2).

After the addition of the base, new ions with m/z 626 were detected, which most probably correspond to the iminium ions formed from the reaction between the catalyst and the product.

The structure of these ions was checked in the CID experiment (Figure 3b). The fragmentation of the ions with m/z 626 isolated from the reaction mixture is identical to the fragmentation of the isobaric ions generated from a solution of the catalyst and the product. The CID spectrum of ions with m/z 626 can be interpreted in the same manner as that discussed above. We can see the elimination of the diphenyltrimethylsilyloxymethyl group (peaks at m/z 255 and 371) and the subsequent fragmentation of the iminium part of the ion, which corresponds to the elimination of fragments with masses of 73 and 172 Da (see Scheme S2 and Figure S5 in the Supporting Information).

Hence, we can characterize iminium ions formed by the reaction between the catalyst and the reactant or the product. For the resolution of the reaction mechanism, it would be advantageous to detect some intermediates on the way from the reactants to the products. Therefore, we have searched for complexes containing both reactants and the catalyst before the elimination of the bromine anion. The only ions corresponding to this requirement are those with m/z 706. These ions can be detected, although only in a very low abundance. The CID spectrum shows elimination of intact diethyl 2-(2-bromoethyl)-malonate, and the remaining peaks correspond to the fragmentation of the iminium ion catalyst/cinnamaldehyde (see Scheme S3 in the Supporting Information). Elimination of HBr, which would correspond to the reaction observed in the solution, is observed with a negligible abundance. This is in agreement with the view that the cyclization reaction step proceeds in a neutral state and that protonation preferentially catalyzes the backward reaction toward the reactants. Figure 1 shows the suggested reaction mechanism, and the species detected by ESI-MS are denoted with their m/z ratios. We note that analogous experiments with diethyl 2-(3-bromopropyl)-

dx.doi.org/10.1021/jo4022106 | J. Org. Chem. 2014, 79, 1563−1570

malonate did not show formation of the product complexes, which is in agreement with the synthetic experiment where no product formation was observed.

We tried to follow the kinetics of the investigated reaction by sampling the reaction mixture by ESI-MS. Although we verified that we can monitor the relative concentrations of cinnamaldehyde and the cyclopentane products by their iminium ions with the catalysts, the results were hardly reproducible. The difficulties during the experiments mainly originated from the formation of an insoluble salt during the reaction (triethylammonium bromide). Although the amount of the salt during short reaction times does not significantly perturb the ESI-MS experiments, on longer time scales, it leads to blocking of the capillary and thus to the instability of the ion signals.

Alternatively, we decided to monitor the kinetics by ^{1}H NMR spectroscopy. Nevertheless, the problems with the formation of the insoluble salt also compromised the NMR results. In addition, longer reaction times led to a significant complexity of the reaction mixture. It was, therefore, problematic to follow the reaction to several half-lives in order to obtain a reliable rate constant, and we had to turn to the determination of the initial-rate kinetics.[20] To this end, we monitored the reaction progress to only the first few percent of the conversion, which avoided the complications that arose during the longer reaction time.

In the initial-rate kinetics approach, we began with eq 1

$$\frac{d[P]}{dt} = -\frac{d[R]}{dt} = k[R] \sim k[R]_0 \quad (1)$$

where $[P]$ is the concentration of the product and $[R]$ is the concentration of the reagent.

In the beginning of the reaction, we can assume that $[R] = [R]_0$. This means that plotting $[P]/[R]_0$ versus t over the first few percent of the reaction gives a line whose slope is k.

During the NMR experiments, the reaction was performed in toluene-d_8 as the solvent. The NMR spectra were acquired for 60 min at given time intervals (Figures S6, S7, 4, and Table 1).

Table 1. Rate Constants Determined from the Initial-Rate Kinetics at Different Temperatures

T (°C)	k (s^{-1} 10^{-5})	$1/T$ (K^{-1})	ln k
25	1.31 ± 0.01	0.0034	−11.2
40	1.49 ± 0.03	0.0032	−11.1
50	2.80 ± 0.08	0.0031	−10.5
60	3.61 ± 0.06	0.0030	−10.2

We tried to reduce the delay in collecting the data at the beginning of the experiment, but some delay was unavoidable because of the (i) mixing of the solution, (ii) initial tuning of the NMR spectrometer after the insertion of a tube with the solution, and (iii) temperation of the solution in the experiments at elevated temperature.

The evaluation of the results according to the Arrhenius equation lead to E_a = 25 ± 7 kJ mol^{-1}. The alternative Eyring equation gives an activation enthalpy of 23 ± 7 kJ mol^{-1} and activation entropy of −263 ± 21 J mol^{-1} K^{-1}, which leads to $\Delta G^{\ddagger}$ (298.15) = 101 ± 9 kJ mol^{-1}.

Our simple approach and derivation of the activation energy/enthalpy is based on the assumption that with the given concentrations of all reactants the initial kinetics is determined by one rate-determining step. We assume that the iminium ions formed from the catalyst and cinnamaldehyde are formed in a fast pre-equilibrium reaction. Similarly, deprotonation of the malonate reactant is controlled by a pre-equilibrium reaction. Coupling of the iminium cations with the anions generated from the malonate reactants is controlled by diffusion (see the following section). Hence, for the analysis, we assumed that the rate-determining step is the cyclization to form the cyclopentane product (as an iminium ion with the catalyst).

Theoretical Calculations. For the theoretical investigation of the title reaction, DFT methods were used. We used the B97D[21,22] functional with empirical correction of dispersion interactions, the M06-2X[23] functional optimized to describe systems reliably in which dispersion interactions play a role, and the B3LYP[24−27] functional because it has been the standard approach for computational investigations of organic reactions in the past. Although the B97D and M06-2X methods lead to qualitatively similar results, the B3LYP method predicts that the initial coupling of iminium ion **1**$^+$ with the anion generated from the malonate reactant is endothermic (Table 2). This is probably because of an underestimation of the stabilization of neutral intermediates **2** by dispersion interactions. Because the calculations using the B97D functional are much faster than those using M06-2X, we decided to use B97D for the optimization of the structures. The energies discussed below correspond either to the B97D/TZVP energies in the gas phase at 0 K or to the B97D/TZVP Gibbs energies calculated with the SMD solvation model at 298.15 K.

Two central steps were investigated in detail: (1) the addition of C-deprotonated diethyl 2-(2-bromoethyl)malonate to the primary iminium ion **1**$^+$ formed from the reaction between the catalyst and cinnamaldehyde (Scheme 2) and (2) the cyclization reaction (Figure 5). The first question we addressed is the structure of the primary adduct **1**$^+$. The most stable isomer has both of the double bonds of the adduct in the trans configuration (**1a**$^+$ in Scheme 2). The isomer with the double bond involving the iminium nitrogen atom in the cis configuration (**1b**$^+$) is 11 kJ mol^{-1} higher in energy. All other isomers are more than 20 kJ mol^{-1} higher in energy. For the following addition reaction step, only structures **1a**$^+$ and **1b**$^+$ were considered.

Addition of C-deprotonated diethyl 2-(2-bromoethyl)-malonate to adduct **1a**$^+$ can proceed either from the *Re* face or the *Si* face of the C−C double bond (blue arrows in Figure 5). According to our calculations, the attack at the *Re* face in the gas phase leads to a slightly more stable intermediate, (*R*)-**2** (the most stable conformer, (*R*)-**2a**, is shown in Figure 5; note that the energies in Figure 5 refer to the CH_2Cl_2 solution and the results for the gas phase are indicated as blue lines for comparison). Diastereoisomer (*S*)-**2** resulting from the *Si*-face attack is about 10 kJ mol^{-1} higher in energy in the gas phase (Table 2). The surprisingly preferred attack from the *Re* face (the face where the bulky pyrrolidine substituent is present) can be explained by the energetically favorable interaction between the bromine atom and hydrogen atoms of the phenyl rings of the pyrrolidine substituent (indicated by the yellow dotted lines in the structure (*R*)-**2a**). The attack from the *Si* face brings the phenyl group of the former cinnamic acid and one of the phenyl groups of the pyrrolidine substituent close to each other. The stabilization of this structure by the possible stacking interaction of the phenyl groups is, however, smaller than that originating from the bromine−phenyl interaction. The situation is, however, changed if we also consider the solvation effect. Taking solvation by CH_2Cl_2 (DCM) into account results in the preference of (*S*)-**2a** by about 10 kJ

dx.doi.org/10.1021/jo4022106 | J. Org. Chem. 2014, 79, 1563−1570

Table 2. Relative Energies of the Intermediates and Transition Structures in the Title Reaction Obtained at Different Levels of Theory[a]

	B97D	B97D PCM	B97D SMD	B3LYP	B3LYP SMD	M06-2X	M06-2X SMD
	$\Delta\Delta H^{0K,GP}$	$\Delta\Delta G^{298K,DCM}$	$\Delta\Delta G^{298K,DCM}$	$\Delta\Delta H^{0K,GP}$	$\Delta\Delta G^{298K,DCM}$	$\Delta\Delta H^{0K,GP}$	$\Delta\Delta G^{298K,DCM}$
1a$^+$ + X(CH_2CH_2Br)$^-$[c]	373	41	25	294	−51	433	76
(*R*)-**2a**	−10	4	10 (0)[b]	−3	−8 (−11)[b]	1	17 (8)[b]
(*R*)-**2b**	6	12	14 (11)[b]	12	14 (4)[b]	20	25 (23)[b]
(*S*)-**2a**	0	0	0 (0)[b]	0	0 (0)[b]	0	0 (0)[b]
(*S*)-**2b**	16	18	22 (22)[b]	24	50 (37)[b]	29	46 (32)[b]
TS_R	67	39	46 (39)[b]	89	72 (65)[b]	125	100 (93)[b]
TS_S	55	31	36 (28)[b]	68	54 (46)[b]	113	90 (82)[b]
(*R*,*R*)-**3**$^+$ + Br^-	320	−63	−39	319	−37	334	−29
(*S*,*S*)-**3**$^+$ + Br^-	281	−87	−62	282	−54	296	−48
1a$^+$ + X($CH_2CH_2CH_2Br$)$^-$[c]	389	47	27	301	−64	444	73
(*R*)-**4a**	−9	−1	1	−18	−7	1	12
(*S*)-**4a**	0	0	0	0	0	0	0
TS_R6	66	47	52	100	83	125	109
TS_S6	75	43	47	101	62	130	101
(*R*,*R*)-**5**$^+$ + Br^-	299	−80	−57	294	−62	312	−43
(*S*,*S*)-**5**$^+$ + Br^-	288	−96	−76	274	−89	301	−61

[a]Energies are given in kJ mol^{-1} relative to the energy of (*S*)-**2a** for the reaction of diethyl (2-bromoethyl)malonate and relative to (*S*)-**4a** for the reaction of diethyl (3-bromopropyl)malonate. Energies were obtained by single-point calculations at the given theory model with the TZVP basis set using geometries optimized at the B97D/6-31g* level of theory either in the gas phase or in CH_2Cl_2 using the PCM solvation model. [b]For comparison with the experimental results, $\Delta\Delta H^{298K,DCM}$ is given in parentheses. [c]X = $CH(COOEt)_2$.

Scheme 2. Possible Isomers of Adduct 1$^+$

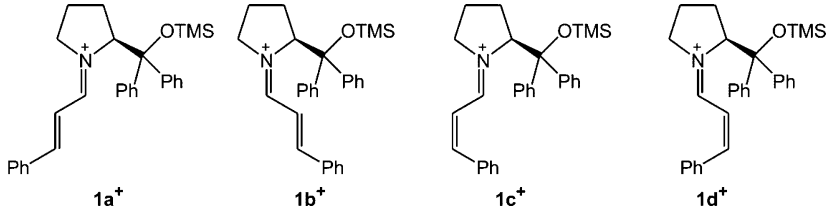

mol^{-1}. We note that the absolute energy differences slightly depend on the theory model used for the calculations. All results can be seen in Table 2.

The reaction between C-deprotonated diethyl 2-(2-bromoethyl)malonate and the less stable isomer **1b**$^+$ leads to the structures of intermediates (*R*)-**2b** and (*S*)-**2b** with relative energies of 14 and 22 kJ mol^{-1}, respectively, with respect to the energy of (*S*)-**2a** (Table 1). The structures can be found in the Supporting Information.

We note that we have also tried to optimize transition structures for the formation of (*R*)-**2a** and (*S*)-**2a**. Because it is a reaction between iminium cation **1**$^+$ and the anion formed by the deprotonation of diethyl 2-(2-bromoethyl)malonate, it is a barrierless process in the gas phase. Nevertheless, even after considering the solvation effect (PCM, CH_2Cl_2), we did not succeed in obtaining the corresponding transition structures. Searching for the transition structure by constrained optimizations led us to conclude that even in the solution the coupling between **1**$^+$ and deprotonated diethyl 2-(2-bromoethyl)malonate is barrierless. Thus, the initial step is probably controlled merely by diffusion of the ions.

The next step after the formation of intermediates (*R*)-**2a** and (*S*)-**2a** corresponds to the cyclization associated with the elimination of the bromine anion. If the reaction proceeds via a S_N2 mechanism, then a particular arrangement with the C═C double bond on the opposite sides of the carbon atom with respect to the leaving bromine anion is required. This arrangement can be only engaged when the bromoethyl group is placed on the opposite side of the plane defined by the C═C double bond and the nitrogen atom of the catalyst with respect to the bulky group of the catalyst. Hence, although this situation is fulfilled for intermediate (*S*)-**2a**, it requires a rotation around C−N bond for intermediate (*R*)-**2a**. This change of conformation leads to the structure of (*R*)-**2b** (i.e., the intermediate formed primarily by the *Re*-side attack of the less stable isomer **1b**$^+$, see earlier), which is 4 kJ mol^{-1} higher in energy than (*R*)-**2a**. The relative energies of the transition structures for the cyclization of (*R*)-**2** and (*S*)-**2** reflect this situation and amount to 46 kJ mol^{-1} (TS_R) and to 36 kJ mol^{-1} (TS_S), respectively. Hence, the activation energies for the cyclization of both intermediates ((*R*)-**2a** and (*S*)-**2a**) are the same with respect to the corresponding reactants, but intermediate (*S*)-**2a** will largely prevail in the reaction mixture and therefore the product of its cyclization ((*S*,*S*)-**3**$^+$) with both new stereocenters in the (S) configuration should preferentially be observed (which is exactly as was found in the experiment).

Comparison of the computational results with the data obtained from the NMR experiments revealed that the M06-2X results best reproduce the experimental value for the Gibbs activation energy. Thus, the NMR kinetics predicts that the

dx.doi.org/10.1021/jo4022106 | J. Org. Chem. 2014, 79, 1563−1570

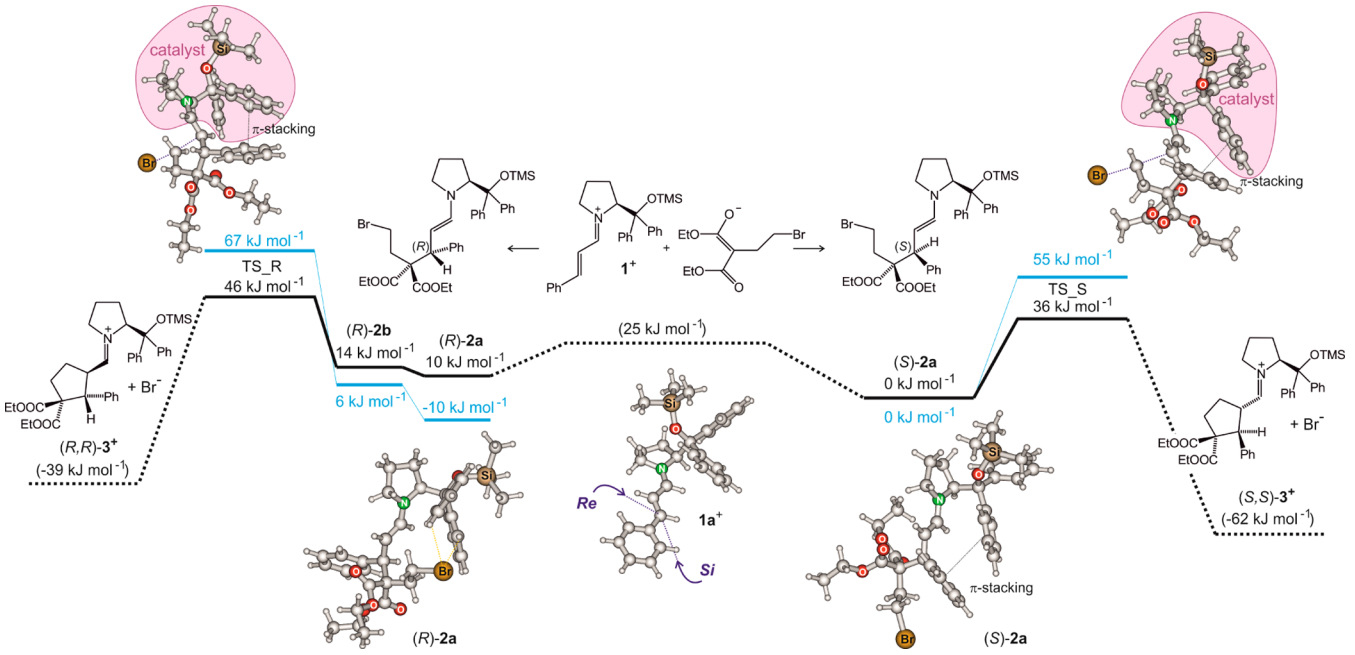

Figure 5. Relative energies ($\Delta\Delta G^{298K,DCM}$) and structures of the intermediates formed by the reaction between adduct $\mathbf{1}^+$ and the anion generated from diethyl 2-(2-bromoethyl)malonate as well as the corresponding transition structures for the cyclization of the intermediates. Results correspond to the calculation at the B97D/TZVP//B97D/6-31g* level of theory using the SMD method for modeling solvation by CH_2Cl_2 (black lines); the results obtained in the gas phase at 0 K are given as blue lines for comparison. Energies for the ionic reactants and products are given in brackets.

Table 3. $\Delta\Delta G^{298K}$ of the Intermediates and Transition Structures in the Title Reaction Obtained at the M06-2X/TZVP Level of Theory Using the SMD Solvation Model[a]

	dioxane	CCl_4	toluene	diethylether	CH_2Cl_2	methanol	acetonitrile	DMF
	ε = 2.210	ε = 2.228	ε = 2.3741	ε = 4.240	ε = 8.930	ε = 32.613	ε = 35.688	ε = 37.219
(*R*)-**2a**	12	13	13	15	17	19	19	19
(*R*)-**2b**	23	24	24	25	25	18	26	26
(*S*)-**2a**	0	0	0	0	0	0	0	0
(*S*)-**2b**	45	45	45	46	46	48	46	46
TS_R	111	111	110	104	100	98	96	96
TS_S	100	100	99	94	90	91	87	87

[a]Energies are given in kJ mol^{-1} relative to the energy of (*S*)-**2a** for the reaction of diethyl (2-bromoethyl)malonate. Energies were obtained by single-point calculations using geometries optimized at the B97D/6-31g* level of theory using the PCM solvation model.

Gibbs activation energy is in the range of 100 kJ mol^{-1}, whereas the M06-2X method provides a value of 90 kJ mol^{-1} in CH_2Cl_2. If we consider activation enthalpies, which are derived on the order of 23 kJ mol^{-1} from the NMR experiments, then the B97D results fit the experiment best. All of the methods tested here, however, lead to analogous conclusions about the reaction mechanism of the title reaction.

Next, we investigated the solvent effect. Because the best agreement with the experiment was obtained with M06-2X functional, we will use the results obtained at this level of theory for the following discussion (Table 3). Experimentally, the best results in terms of conversion and stereoselectivity were obtained for the reaction in toluene, whereas the reaction did not proceed at all in methanol and dimethylformamide (DMF).[8] Nevertheless, the polarity of the solvent is not the only property that plays a role because the reaction proceeds in acetonitrile with similar *ee* values as observed for all other less-polar solvents.[28]

The calculations show that with the increasing polarity of the solvents the energy discrimination between intermediates (*R*)-**2** and (*S*)-**2** becomes larger and the barriers for the cyclization become smaller. Hence, in principle, the more polar the solvent, the more selective and faster the reaction should be. The origin of the effect of the solvent is in the increasingly better solvation of the transition structures compared to the primary adduct intermediates, which stems from the fact that the transition structures are more polarized than the intermediates (it involves a transition from the neutral intermediate to the ionic products).

The effect of the solvents on the potential energy surface of the cyclization step does not explain the solvent effects observed in the experiment. Therefore, we also have to take into account other parts of the reaction. For example, intermediates (*R*)-**2** and (*S*)-**2** are formed in the reaction between two ions (positively charged $\mathbf{1}^+$ reacts with an anion formed from the malonate reactant). This reaction step will be increasingly disfavored with the increasing polarity of the solvent because polar solvents will stabilize the ions. Hence, undesired reaction channels starting at the stage of the ionic reactants are probably responsible for the observed solvent effect of methanol and DMF rather than the effect on the cyclization reaction itself. In agreement with this, for the

dx.doi.org/10.1021/jo4022106 | J. Org. Chem. 2014, 79, 1563−1570

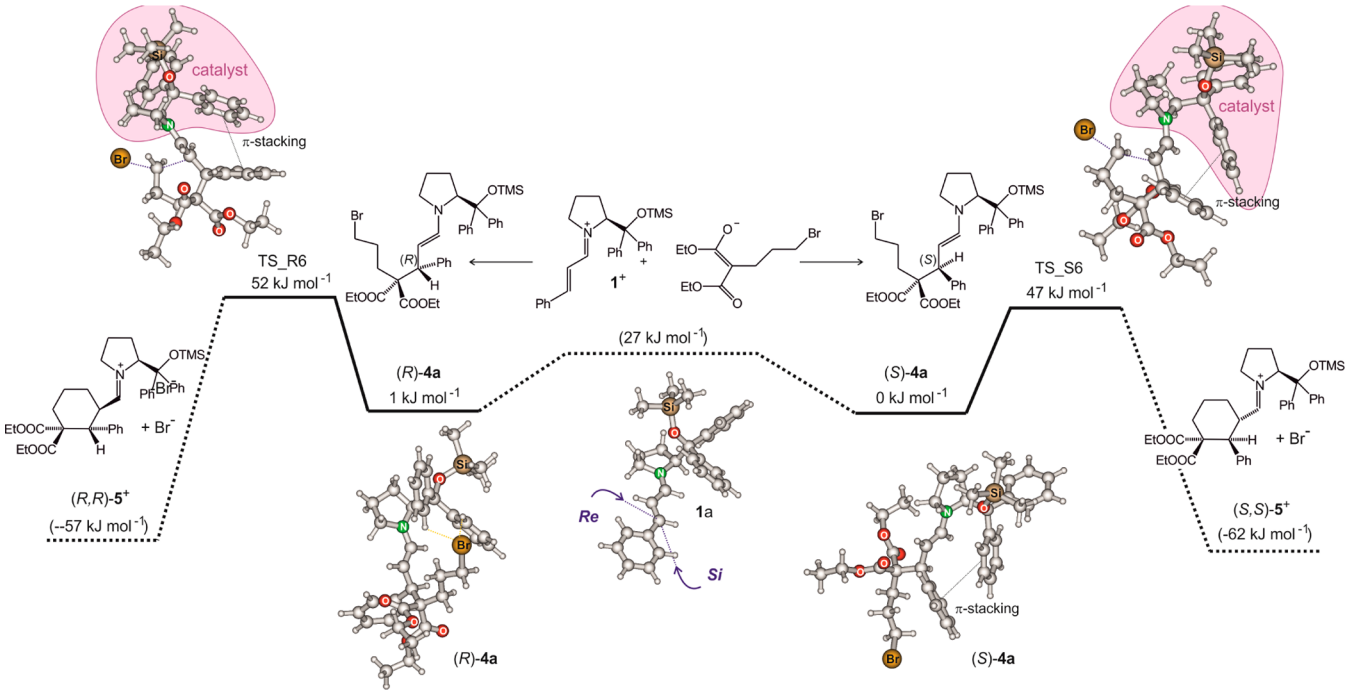

Figure 6. Relative energies ($\Delta\Delta G^{298K,DCM}$) and structures of the intermediates formed by the reaction between adduct $\mathbf{1}^+$ and the anion generated from diethyl 2-(3-bromopropyl)malonate as well as the corresponding transition structures for the cyclization of the intermediates. Results correspond to the calculation at the B97D/TZVP//B97D/6-31g* level of theory using the SMD method for modeling solvation by CH_2Cl_2. Energies for the ionic reactants and products are given in brackets.

reaction in DMF, it was found that the initially formed anions from the malonate reactants undergo self-cyclization to yield diethyl-cyclopropane-1,1-dicarboxylates.[28]

We have further tested the proposed mechanism on the analogous reaction between cinnamaldehyde and diethyl 2-(3-bromopropyl)malonate catalyzed by the same catalyst. It was found experimentally that this reaction does not proceed. Computationally, we have found analogous reaction pathways as those shown in Figure 5 (cf. Figure 6). Formation of the intermediate with the new stereocenter with the (R) configuration ((*R*)-**4**) is favored in the gas phase by 9 kJ mol^{-1} with respect to the intermediate having the new stereocenter in the (S) configuration ((*S*)-**4**) (results at the B97D level of theory). Transfer to the CH_2Cl_2 solution results in almost the same relative energies for both stereoisomers (Table 2).

Relative energies of the reaction barriers for the cyclization of (*R*)-**4** or (*S*)-**4** are about 10 kJ mol^{-1} higher than those found for the smaller system at all levels of theory used. The energy differences for the formation of the two expected diastereoisomeric products, (*R*,*R*)-$\mathbf{5}^+$ and (*S*,*S*)-$\mathbf{5}^+$, are slightly smaller than those found for (*R*,*R*)-$\mathbf{3}^+$ and (*S*,*S*)-$\mathbf{3}^+$. Hence, the formation of the six-membered ring should proceed significantly slower than that of the five-membered ring, and in addition, smaller *ee* values would be expected if the reaction proceeded.

CONCLUSIONS

The reaction mechanism of a cascade reaction between cinnamaldehyde and diethyl 2-(2-bromoethyl)malonate catalyzed by *O*-trimethylsilyldiphenylprolinol was investigated. Using ESI-MS, the primary iminium adduct between the aldehyde and the catalyst was identified as well as the formation of the product adduct with the catalyst. The intermediate formed by the addition of an anion generated from diethyl 2-(2-bromoethyl)malonate to the primary iminium adduct is neutral and therefore could have been detected only as the protonated form. The activation barriers were determined from NMR experiments as E_a = 25 ± 7 kJ mol^{-1} (Arrhenius equation) or $\Delta H^{\ddagger}$ = 23 ± 7 kJ mol^{-1} (Eyring equation). The final Gibbs activation energy amounts to 101 ± 9 kJ mol^{-1}. The theoretical results confirm that the intuitive mechanism considered for this type of reaction is correct. In detail, it shows that the relative stabilities of the two stereoisomers of the primary iminium adduct depend on the solvent. The energy barriers for the cyclization of the primary adducts reflect their relative energies. The energy discrimination between the two primary stereoisomers is therefore crucial for the overall stereoselectivity of the reaction. We found that the more polar the solvent is, the larger the energy discrimination between the primary adducts and the lower the energy barriers for the cyclization. Nevertheless, more polar solvents will discriminate in the formation of the primary adduct and thus allow side reactions. The experimentally observed solvent effects will therefore reflect the interplay between these two concurring trends.

EXPERIMENTAL DETAILS

Chemicals. The catalyst ((*S*)-(−)-α,α-diphenyl-2-pyrrolidinemethanol trimethylsilyl ether), cinnamaldehyde, triethylamine, and toluene-d_8 were purchased from Sigma-Aldrich and used without further purification. Dichloromethane of p.a. quality was used. Malonate was prepared in two steps from diethylmalonate with 1,2-dibromoethane, leading to diethyl 1,1-cyclopropanedicarboxylate according to a literature method,[29] and the cyclopropane ring was opened by HBr(g) according to a literature method.[30]

Mass Spectrometric Experiments. The experiments were performed with a TSQ Classic mass spectrometer, which has been described previously.[31] Briefly, the TSQ Classic consists of an electrospray ionization (ESI) source combined with a tandem mass

dx.doi.org/10.1021/jo4022106 | J. Org. Chem. 2014, 79, 1563−1570

spectrometer of QOQ configuration (Q stands for quadrupole and O for octopole). The investigated ions were generated by ESI using a 5 mM solution of cinnamaldehyde in CH_2Cl_2 with 20 mol % of the catalyst (DPPTMS), 1.1 equiv of diethyl 2-(2-bromoethyl)malonate, and 1.3 equiv of triethylamine. The first quadrupole was used as a mass filter to scan the spectrum of the ions produced upon ESI or to select particular ions of interest. The Q1-selected ions were then guided through the octopole serving as a collision chamber followed by mass analysis of the ionic reaction products by means of the second quadrupole and subsequent detection. The collision gas (Xe) was leaked into the octopole at typical pressures on the order of 10^{-4} mbar. The origin of the collision-energy scale was determined using retarding potential field analysis.[31] The MS^n experiments (shown in the Supporting Information) were performed with a Finnigan LCQ ion trap mass spectrometer equipped with an ESI source.[32]

The ^1H NMR data were recorded using a Varian Inova (400 MHz) NMR spectrometer for the experiments at 40, 50, and 60 °C and a Bruker Avance III (600 MHz) NMR spectrometer for the experiment at 25 °C. The reaction mixtures were prepared as follows: 47 mg (1 equiv) of cinnamaldehyde was mixed with 24 mg (0.2 equiv) of chiral catalyst (*S*)-DPPTMS, 104 mg (1 equiv) of diethyl 2-(2-bromoethyl)-malonate, and 24 g (1.3 equiv) of triethylamine in 1 mL of toluene-d_8, and the mixture was immediately introduced into the NMR instrument. The representative spectra of the reaction mixtures are shown in the Supporting Information, Figures S6 and S7.

Computational Details. All structures reported here were optimized using the B97D functional,[21,22] which includes a semi-empirical correction for dispersion interaction (DFT-D), as implemented in the Gaussian 09 suite.[33] The interactions between the phenyl substituents of the pyrrolidine catalyst and the reactant may play an important stabilization role; therefore, the inclusion of dispersion interactions might be decisive for the correct description of the entire system.[34] With respect to the size of the studied system, the geometry optimizations and thermochemistry calculations were performed at the B97D/6-31G* level of theory, and the final energies of the most stable structures identified were determined by single-point calculations at the B97D/TZVP level as well as at the B3LYP/TZVP[24−27] and M06/TZVP[23] levels for comparison (Table 2). All minima and transition states were further reoptimized again at the B97D/6-31G* level of theory using the polarized continuum model for modeling the effect of solvent;[35] frequency calculations were again performed to control the identity of the stationary points as well as to obtain thermochemical corrections for Gibbs energies at 298 K, and the final energies were again obtained by single-point calculations at the B97D/TZVP, B3LYP/TZVP, and M06/TZVP levels using the SMD solvation model.[36]

■ ASSOCIATED CONTENT

Ⓢ Supporting Information

MS^n spectra, suggested fragmentation schemes of selected ions, representative NMR spectra, and computed Cartesian coordinates of all of the molecules reported in this study (the file containing the coordinates may be opened as a text file or imported to a molecular modeling program for visualization). This material is available free of charge via the Internet at http://pubs.acs.org.

■ AUTHOR INFORMATION

Corresponding Author

*E-mail: roithova@natur.cuni.cz.

Notes

The authors declare no competing financial interest.

■ REFERENCES

(1) For reviews on organocascade reactions (including iminium-enamine sequence), see: (a) Pellissier, H. *Adv. Synth. Catal.* **2012**, *354*, 237. (b) Moyano, A.; Rios, R. *Chem. Rev.* **2011**, *111*, 4703. (c) Alba, A.-N.; Companyo, X.; Viciano, M.; Rios, R. *Curr. Org. Chem.* **2009**, *13*, 1432. (d) Enders, D.; Grondal, C.; Huettl, M. R. M. *Angew. Chem., Int. Ed.* **2007**, *46*, 1570.

(2) Ibrahem, I.; Zhao, G.-L.; Rios, R.; Veselý, J.; Sunden, H.; Dziedzic, P.; Cordova, A. *Chem.—Eur. J.* **2008**, *14*, 7867.

(3) Rios, R.; Vesely, J.; Sunden, H.; Ibrahem, I.; Zhao, G.-L.; Cordova, A. *Tetrahedron Lett.* **2007**, *48*, 5835.

(4) Zu, L.; Li, H.; Xie, H.; Wang, J.; Jiang, W.; Tang, Y.; Wang, W. *Angew. Chem., Int. Ed.* **2007**, *46*, 3732.

(5) Wang, J.; Li, H.; Xie, H.; Zu, L.; Shen, X.; Wang, W. *Angew. Chem., Int. Ed.* **2007**, *46*, 9050.

(6) Enders, D.; Wang, C.; Bats, J. W. *Angew. Chem., Int. Ed.* **2008**, *47*, 7539.

(7) Ma, A.; Ma, D. *Org. Lett.* **2010**, *12*, 3634.

(8) Remeš, M.; Veselý, J. *Eur. J. Org. Chem.* **2012**, 3747.

(9) Chen, P. *Angew. Chem., Int. Ed.* **2003**, *42*, 2832.

(10) Roithová, J.; Janková, Š.; Jašíková, L.; Váňa, J.; Hybelbauerová, S. *Angew. Chem., Int. Ed.* **2012**, *51*, 8378.

(11) Jašíková, L.; Hanikýřová, E.; Škríba, A.; Jašík, J.; Roithová, J. *J. Org. Chem.* **2012**, *77*, 2829.

(12) Ducháčková, L.; Kadlčíková, A.; Kotora, M.; Roithová, J. *J. Am. Chem. Soc.* **2010**, *132*, 12660.

(13) Santos, L. S.; Pavam, C. H.; Almeida, W. P.; Coelho, F.; Eberlin, M. N. *Angew. Chem., Int. Ed.* **2004**, *43*, 4330.

(14) Maltsev, O. V.; Chizhov, A. O.; Zlotin, S. G. *Chem.—Eur. J.* **2011**, *17*, 6109.

(15) Schrader, W.; Handayani, P. P.; Zhou, J.; List, B. *Angew. Chem., Int. Ed.* **2009**, *48*, 1463.

(16) Zhang, G. C.; Wang, Y. F.; Zhang, W.; Xu, X. S.; Zhong, A. G.; Xu, D. Q. *Eur. J. Org. Chem.* **2011**, 2142.

(17) Fleischer, I.; Pfaltz, A. *Chem.—Eur. J.* **2010**, *16*, 95.

(18) Tang, J.; Xu, D. Q.; Xia, A. B.; Wang, Y. F.; Jiang, J. R.; Luo, S. P.; Xu, Z. Y. *Adv. Synth. Catal.* **2010**, *352*, 2121.

(19) Marquez, C. A.; Fabbretti, F.; Metzger, J. O. *Angew. Chem., Int. Ed.* **2007**, *46*, 6915.

(20) For selected mechanistic studies using NMR, see: (a) Zuend, S. J.; Jacobsen, E. N. *J. Am. Chem. Soc.* **2009**, *131*, 15358. (b) Zhu, J.-L.; Zhang, Y.; Chong, L.; Zheng, A.-M.; Wang, W. *J. Org. Chem.* **2012**, *77*, 9813. (c) Susanne, F.; Smith, D. S.; Codina, A. *Org. Process Res. Dev.* **2012**, *16*, 61. (d) Vilhelmsen, M. H.; Jensen, J.; Tortzen, Ch. G.; Nielsen, M. B. *Eur. J. Org. Chem.* **2013**, 701.

(21) Grimme, S. *J. Comput. Chem.* **2006**, *27*, 1787.

(22) Pevarati, R.; Baldridge, K. K. *J. Chem. Theory Comput.* **2008**, *4*, 2030.

(23) Zhao, Y.; Truhlar, D. G. *Theor. Chem. Acc.* **2008**, *120*, 215.

(24) Vosko, S. H.; Wilk, L.; Nusair, M. *Can. J. Phys.* **1980**, *58*, 1200.

(25) Lee, C.; Yang, W.; Parr, R. G. *Phys. Rev. B* **1988**, *37*, 785.

(26) Becke, A. D. *Phys. Rev. A* **1988**, *38*, 3098.

(27) Becke, A. D. *J. Chem. Phys.* **1993**, *98*, 5648.

(28) Remeš, M.; Géant, P. Y.; Putaj, P.; Šebestík, J.; Císařová, I.; Roithová, J.; Veselý, J. *Adv. Synth. Catal.*, submitted for publication.

(29) Dmowski, W.; Wolniewicz, A. *J. Fluorine Chem.* **2000**, *102*, 141.

(30) Steffen, K.-D. U.S. Patent 5,463,111, 1995.

(31) Ducháčková, L.; Roithová, J. *Chem.—Eur. J.* **2009**, *15*, 13399.

(32) Kumar, P.; Roithova. *Eur. J. Mass Spectrom.* **2012**, *18*, 457.

(33) Frisch, M. J.; et al. *Gaussian 09*, revision A.02; Gaussian, Inc.: Wallingford, CT, 2009.

(34) Hobza, P.; Müller-Dethlefs, K. *Non-Covalent Interactions: Theory and Experiments*; RSC: London, 2010.

(35) Tomasi, J.; Mennucci, B.; Cammi, R. *Chem. Rev.* **2005**, *105*, 2999.

(36) Marenich, A. V.; Cramer, C. J.; Truhlar, D. G. *J. Phys. Chem. B* **2009**, *113*, 6378.